Molecular Immunology 105 (2019) 96–106

Contents lists available at ScienceDirect

Molecular Immunology

journal homepage: www.elsevier.com/locate/molimm

Magnolol attenuates the inflammation and enhances phagocytosis through the activation of MAPK, NF-κB signal pathways *in vitro* and *in vivo*

Hongce Chen[a,1], Wuyu Fu[a,1], Hongyuan Chen[a,c,d,1], Siyuan You[a], Xiawan Liu[a], Yujiao Yang[e], Yao Wei[e], Jun Huang[f], Wen Rui[b,d,e,*]

[a] Department of Immunology, Institute of Basic Medical Sciences, Guangdong Pharmaceutical University, Guangzhou, 510006, PR China
[b] Centre Laboratory, Guangdong Pharmaceutical University, Guangzhou, 510006, PR China
[c] Guangdong Engineering & Technology Research Center of Topical Precise Drug Delivery System, Guangdong Pharmaceutical University, Guangzhou, 510006, PR China
[d] Key Laboratory of Digital Quality Evaluation of Chinese Materia Medica of State Administration of TCM, Guangzhou, 510006, PR China
[e] School of traditional Chinese medicine, Guangdong Pharmaceutical University, Guangzhou, 510006, PR China
[f] Key Laboratory of Immunology, Sino-French Hoffmann Institute, Guangdong Provincial Key Laboratory of Allergy & Clinical Immunology, School of Basic Medical Sciences;Guangzhou Medical University, Guangzhou 511436, P. R. China

ARTICLE INFO

Keywords:
Magnolol
Phagocytosis
MAPK
NF-κB
Signaling pathway
Inflammatory bowel disease

ABSTRACT

Magnolol is a natural extract and the main bioactive component from Chinese medicine-Magnolia. We speculate that it's functional action might be associated with the anti-inflammatory effects of magnolol. Herein, the main purpose was to elucidate the phagocytic immune function and anti-inflammatory activities associated. The toxicity of magnolol on U937 and LO-2 cells was assayed by MTT, flow cytometry and laser scanning confocal microscope was utilized to detect the phagocytosis effect on U937 cells, C57BL/6 mice and the follow-up hematoxylin-eosin staining methods were used to evaluate its bioactivity *in vivo*. The results showed that magnolol had dose dependent effects on enhancement of phagocytosis ability and significantly inhibited the NO production at the concentration range from10 to 40 μM. Furthermore, Magnolol significantly reduced the gene expression and protein release of IL-1β and TNF-α. However, the p-ERK1/2 in MAPK signaling pathway was not significantly affected by magnolol, whereas p-JNK and p-P38 were down-regulated. Magnolol also inhibited the expression of p-IκBα and p-P65 of NF-κB signaling pathways. The loss of body weight and the shorter length of colon were significantly improved in DSS-treated colitis C57BL/6 mice after the administration of magnolol. The cytokines of pro-inflammatory factors TNF-α, IL-6 and IL-1β attenuated significantly in a concentration dependent manner. The histopathological manifestations of 5–20 mg/kg after the treatment magnolol were markedly improved in the DSS-treated mice. These findings showed that magnolol exerted an anti-inflammatory effect through immunoregulatory phagocytosis, MAPK and NF-κB signaling pathways. Our results provide experimental evidence and theory basis for research on anti-inflammatory effects for magnolol as a potentially anti-inflammatory drug candidate.

1. Introduction

Magnolia officinalis, a green plant with the bark contains magnolol and honokiol two compounds, is widely used in China and other Asian countries as a traditional Chinese medicine. Preclinical studies have evaluated their various potential applications including anti-oxidant, anti-bacterial, anti-viral, anti-tumor, anti-asthma, cardiovascular protection (Wang et al., 2000; Zhao et al., 2017; Pang et al., 2013),

Abbreviations: MTT, methyl thiazolyl tetrazolium; LSCM, laser scanning confocal microscope; NO, Nitric oxide; ELISA, enzyme linked immunosorbent assay; IL-1β, interleukin-1β; TNF-α, tumor necrosis factor-α; COX-2, cyclooxygenase-2; iNOS, nitric oxide synthase; RT-PCR, real-time polymerase chain reaction; MAPK, mitogen-activated protein kinase; ERK, extracellular-signal regulated protein kinase; SAPK, stress-activated protein kinase; BMK, big MAP kinase; SAIDs, steroidal anti-inflammatory drugs; NSAIDs, nonsteroidal anti-inflammatory drugs; FBS, fetal bovine serum; LPS, lipopolysaccharide; FITC, fluorescein isothiocyanate; DMSO, dimethyl sulfoxide; SDS-PAGE, sodium dodecyl sulphate polyacrylamide gel electrophoresis; BCA, bicinchoninic acid; OD, optical delnsity; PBS, phosphate buffer saline; DXM, dexamethasone; Ct, threshold cycle; HRP, horseradish peroxidase; GAPDH, glyceraldehyde-3-phosphatedehydrogenase; DAI, disease activity index; PVDF, polyvinylidene difluoride

* Corresponding author at: Centre Laboratory, Guangdong Pharmaceutical University, Guangzhou, 510006, PR China.
E-mail address: gyrw@gdpu.edu.cn (W. Rui).

[1] These authors contributed equally to this paper.

https://doi.org/10.1016/j.molimm.2018.11.008
Received 19 September 2018; Received in revised form 22 October 2018; Accepted 11 November 2018
Available online 27 November 2018

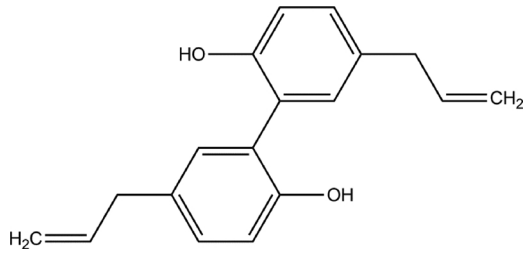

Fig. 1. The chemical structure of magnolol (IUPAC name 4-Allyl-2-(5-allyl-2-hydroxy-phenyl) phenol, Molecular-weight: 266.33, formula: C18H18O2).

Magnolol (Fig. 1), a major phenolic compound with bioactivity purified from Magnolia officinalis. However, Whether magnolol regulates immune phagocytosis, its anti-inflammatory effects and molecular mechanisms are unknown.

Phagocytosis, an immunoregulatory mechanism of endocytosis in cells, pledges support to ingest substances that fail to enter cells through transmembrane. It is often occurred during inflammation. The ingestion process is essential for immune responses during the clearance of apoptotic cells and successful host defense. Macrophages express numbers of antigenic receptors in cell surface which widely recognize tumor cells and other foreign bodies to kill them directly or through secreting related cytokines and cytotoxic substances (Doherty and Mcmahon, 2009; Rabinovitch, 1995). Besides phagocytosis, macrophages, a type of white blood cell, play a critical role in nonspecific defense and also help initiate specific defense mechanisms by recruiting other immune cells(Ovchinnikov, 2010). NO is an important cell messenger molecule and toxic factor, and promotes the apoptosis of macrophages at high concentration (Farghadan et al., 2016). In the immunological or inflammatory disease animal models, the concentration of NO was significantly increased in the lesions and the experimental animal symptoms were improved by inhibiting the production of NO (Park and Song, 2017, Wang et al.,2017).

Macrophages are a major component of the mononuclear phagocyte system that consists of closely related cells of bone marrow origin, including blood monocytes, and tissue macrophages. From the blood, monocytes migrate into various tissues and transform macrophages. In inflammation, macrophages have three major function; antigen presentation, phagocytosis, and immunomodulation through production of various cytokines and growth factors. Macrophages play a critical role in the initiation, maintenance, and resolution of inflammation. They are activated and deactivated in the inflammatory process. Activation signals include cytokines (interferon γ, granulocyte-monocyte colony stimulating factor, and tumor necrosis factor α), bacterial lipopolysaccharide, extracellular matrix proteins, and other chemical mediators. Inhibition of inflammation by removal or deactivation of mediators and inflammatory effector cells permits the host to repair damages tissues. Activated macrophages are deactivated by anti-inflammatory cytokines (interleukin 10 and transforming growth factor ß) and cytokine antagonists that are mainly produced by macrophages. Macrophages participate in the autoregulatory loop in the inflammatory process. Because macrophages produce a wide range of biologically active molecules participated in both beneficial and detrimental outcomes in inflammation, therapeutic interventions targeted macrophages and their products may open new avenues for controlling inflammatory diseases (Fujiwara and Kobayashi, 2005). Inflammation, a common clinical pathology process, is the immune defense response to exogenous pathogens invasion. Inflammatory cells can recruit immune cells in large quantities which will promote the activation of endothelial cells and dormant tumor cells to promote the development of tumor (Park et al., 2011; Fong et al., 1990; Hansson, 2005; Gabay and Kushner, 1999). Nowadays, the most important signaling pathways in the inflammatory process are MAPK and NF-κB. MAPK, including ERK, p38MAPK, SAPK/c-Jun/JNK and BMK1/ERK5 four subfamilies, is one of the extremely important signal transduction pathways and involves in the growth, differentiation, apoptosis, immune regulation, wound healing and other physioloial and pathological processes of cells (Robinson and Cobb, 1997; Huang et al., 2009). NF-κB, a dimer transcription factor, is composed of isotype or hetero rel family protein from p50 and p65 composition(Lawrence et al., 2001). NF-κB plays an important role in the process of immunization, inflammation, apoptosis, tumor occurrence and other biological processes through regulating the expression of inflammatory factors, chemokines, growth factors, COX-2, iNOS and so on (Killeen et al., 2014).

Herin, our hypothysis of its immunoregulatory and anti-inflammatory effects might associate with magnolol. The follow-up experiments were carried on for investigation the anti-inflammatory molecular mechanism *in vitro* and the anti-inflammatory activity *in vivo*.

2. Materials and methods

2.1. Materials and regents

Magnolol with purity 98.8% was purchased National Institutes for Food and Drug Control, People's Republic of China (Batch number : 110729-201513) (Beijing,China), 1640 and FBS were from Gibco (Carlsbad, CA, USA),LPS, DMSO, MTT, β-mercaptoethanol, Ammonium persulfate, Methylene diacrylamide, Acrylamide, DSS, Hematoxylin and Eosin were purchased from Sigma Aldrich (St. Louis, MO. USA), Annexin V-FITC/PI Kit was obtained from KeyGen BioTECH (Nanjing, China), Penicillin/streptomycin was purchased from Huashun BioTECH (Shanghai, China), Trypsin and EDTA were obtained from Amresco (Solon, OH, USA), SDS, PMSF, DEPC, 4% paraformaldehyde, Skim milk powder were purchased from Sijia BIOTECH (Guangzhou, China),Trizol was purchased from Invitrogen (Carlsbad, CA, USA), Glycine, Ethanol, Isopropyl alcohol were obtained from Guangzhou Chemical Reagent Factory (Guangzhou, China), Primer was obtained from BGI (Shenzhen, China), Prime ScriptTM RT reagent Kit was purchased from Takara (Kusatsu, Japan), So FastTM EvaGreen Supermix Kit was obtained from BIO-RAD(Hercules, CA, USA),ECL hypersensitive luminescence Kit, BCA protein quantification kit and Tween-20 were purchased from Beyotime (Shanghai, China), goat anti rabbit IgG, goat anti mouse IgG were obtained from Millipore (Billerica, MA, USA), rabbit polyclonal anti-p-ERK1/2, rabbit polyclonal anti-ERK1/2, rabbit polyclonal anti-p-SAPK/JNK, rabbit polyclonal anti-SAPK/JNK, rabbit polyclonal anti-p-p38, rabbit polyclonal anti-p38, mouse polyclonal anti-IκBα, mouse polyclonal anti-p-IκBα, rabbit polyclonal anti-p-NF-κB, rabbit polyclonal anti-NF-κB, rabbit monoclonal anti-GAPDH were obtained from Cell Signaling Technology (Danvers, MA, USA), ELISA Kit for TNF-αwas purchased from Proteintech Group, Inc (Rosemont, IL, USA), ELISA Kit for IL-6 and IL-1βwere obtained from R&D systems (Minneapolis, MN, USA).

2.2. Cells culture and induce differentiation

U937 and LO-2 cells were cultured in 1640 medium at saturated humidity environment and incubated at 37 °C with 5% CO_2. Cells were digested and transferred culture for further experiments when the density of cells reached 80–90%. The logarithmic growth phase cells of U937 were collected and cultured in 1640 inductive medium and the density was adjusted to 2.5×10^5 cells/mL. Cells were seeded in the corresponding cell culture dish and induced differentiation into macrophages for 48 h.

2.3. Animals

6-week-old female C57BL/6 mice were obtained from Guangdong province medical laboratory animal center, People's Republic of China (Certification : 44,007200046895).Our protocol conforms with guide for the care and use of laboratory animals published by the US National

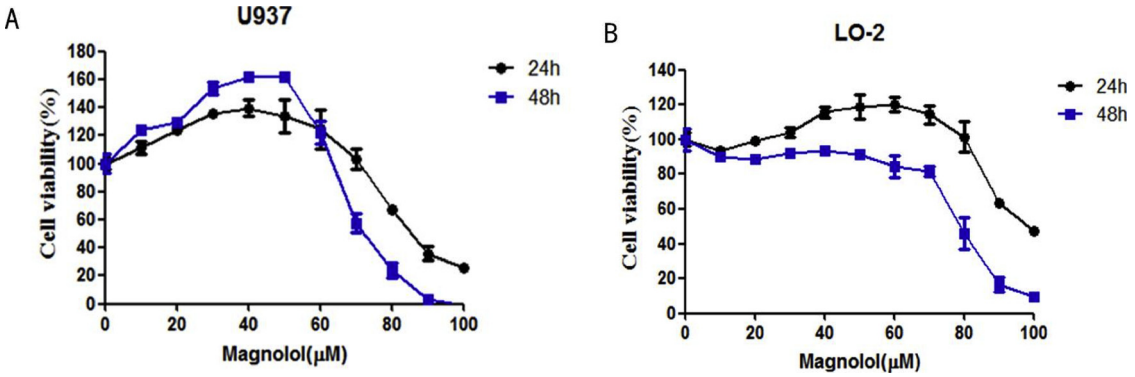

Fig. 2. Cytotoxicity of magnolol on U937 and LO-2 cells. Cell viability of U937 (A) and LO-2 (B) were measured by MTT after treated with magnolol. All data were expressed as the mean ± SD, n = 4.

Table 1
Effects of magnolol on U937 cells phagocytosis ($\bar{x}$ ± s. n = 6).

	Control	Magnolol(μM)			
		1	10	20	40
Phagocytic rates (%)	44.67 ± 2.94	48.47 ± 4.21	52.27 ± 2.75*	55.40 ± 5.40*	64.33 ± 4.50**

* P < 0.05 versus Control group.
** P < 0.01 versus Control group.

Institutes of Health(NIH Publication No. 85-23, revised 1996)and was approved by the Ethics Committee of Guangdong Pharmaceutical University Animal Center.

2.4. Measurement of Cytotoxicity of Magnolol (Ying et al., 2016, Schroeder et al., 2014)

U937 cells were plated into 96-well plate and induced differentiation. After 48 h, cells were exchanged fresh inductive medium containing magnolol at the final concentration of 10, 20, 30, 40, 50, 60, 70, 80, 90, 100 μM with four wells. 10 μL/well of MTT solution was added to each well, and the cells were continually incubated for 4 h after treated 24 h and 48 h. Then the supernatant was carefully aspirated and 100 μL/well DMSO was added. After incubated at room temperature for 15 min, the absorbance (OD) of each group was measured at 570 nm. Cell viability is calculated as follows: Cell viability (%) = (mean OD of the experiment - mean OD in the control group)/average OD of the control group × 100. Except inducting differentiation, the cytotoxicity of magnolol in LO-2 cells was measured as previously described in U937 cells.

2.5. Flow cytometry analysis and confocal microscopy (Chen et al., 2015; Shao et al., 2015)

U937 cells were inoculated into 60 mm cell culture plates with inductive medium for 48 h. The supernatant was discarded and cells were cultured with 1640 containing magnolol (with the final concentration of 102040 μM, respectively), while the blank and control groups were set. After pretreatment in the incubator for 3 h, 2 mL/plate fluorescent microspheres were added and cells were incubated for 1 h. In the dark condition, the cryopreserved PBS was used to wash cells for 3 times. Cells were collected and centrifuged at 2000 rpm for 5 min. The supernatant was discarded and 4% paraformaldehyde was added to fix cells for 15 min. Centrifuged for 5 min, then discarded the supernatant and washed the cells 3 times with pre-cooling PBS. Finally, the phagocytosis of U937 cells were determined by flow cytometry.

U937 cells were inoculated into confocal cell culture dishes and treated same as above steps. After pretreated for 3 h, cells were cultured with 200 μL/day fluorescent microspheres.

In the dark condition, cells were washed by pre-cooled PBS for 3 times. After added for 15 min, 4% paraformaldehyde fixative was discarded and cells were washed three times with pre-cooled PBS and added 200 μL PBS into pre well. The phagocytosis of U937 cell was detected by laser confocal.

2.6. Construction of U937 cells inflammatory model

Cells were inoculated into suitable plates to induce differentiation for 48 h and then the supernatant was discarded. The model group was supplemented with 1 mL/well 1640 induction medium containing LPS with the final concentration of 100 ng/mL. In the blank group, only 500 μL/1640 induction medium were added and cells were continued to culture for 24 h.

2.7. Determination of NO production induced by LPS in U937

U937 cells were inoculated into 24-well plates to induce differentiation for 48 h, and the supernatant was discarded. In the group of magnolol, Magnolol was added into the 1640 induction medium and the final concentrations of magnolol were 1, 10, 20 μM. Cells were pretreated with the culture medium containing magnolol (final concentration: 0.1, 1, 10, 20, 40 μM) in LPS + magnolol group for 3 h. And the appropriate amount of LPS solution (final concentration of 100 ng/mL) was added to continue to culture for 24 h, while the blank group and the control group were set. The supernatant was collected and centrifuged at 10,000 rpm for 5 min.

According to the instruction of Griess Reagent, 1640 induction medium was used to prepare the standards and the concentration were desirable 0, 1.5625, 3.125, 6.25, 12.5, 25, 50, 100 μM. 50 μL/well of standards and samples from each group were added to the 96-well plate. There were three wells in parallel. An equal volume of Griess A solution and B solution were added and shaken. The microplate reader was irradiated at 540 nm to read absorbance OD values. Standard curve was used to calculate the NO content in the supernatant of each group.

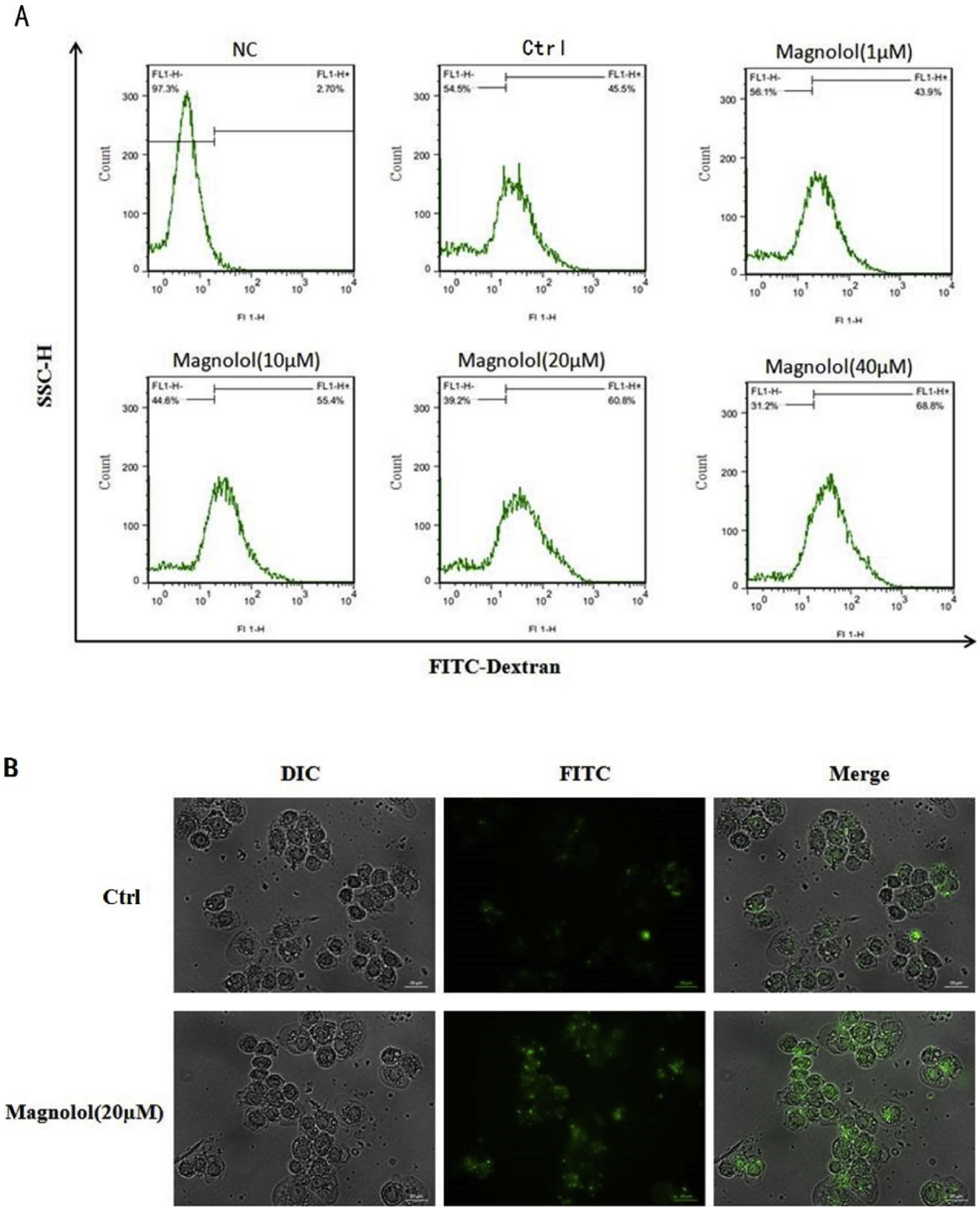

Fig. 3. Magnolol induced phagocytosis on U937 cells (100×). The function of phagocytosis induced by magnolol on U937 cells was detected by flow cytometry(A) and confocal microscope (B). Representative immunofluorescence images were taken.

2.8. Real-time PCR analysis and ELISA analysis

After induced differentiation, the supernatant of U937 was discarded and the 1640 basal medium containing magnolol (10, 20, 40 μM) and DXM (10 μM) was added for 3 h. Then the appropriate amount of LPS solution (100 ng/mL) was added to continue culturing 6 h, while the blank group and the control group were set.

The supernatant of the cells was collected and centrifuged at 10,000 rpm for 5 min, then the precipitate was discarded. Cell supernatant samples were determined using ELISA kits according with the standard procedures recommended.

In brief, the total RNA from U937 was extracted by Trizol, qRT-PCR was performed by Prime ScriptTM RT reagent Kit and SsoFast Eva Green Supermix. The program was running for 30 s at 95 °C, following by 40 cycles of 5 s at 95 °C and 5 s + plate Read at 56 °C and 5 s + plate read at 65–95 °C. The general principles of primers were designed in the Genebank database and the sequences were as follows: IL-1β (Gene ID: NC_000002.12) forward primer, 5′-TGATGGCTTATTACAGTGGCA ATG-3′, IL-1β reverse primer, 5′-GTAGTGGTGGTCGGAGATTCG-3′, TNF-α (Gene ID: NO_000006.12) forward primer, 5′-GGGCCTGTACCT CATCTACT-3′, TNF-α reverse primer, 5′-TGACCTTGGTCTGGTAG GAG-3′, GAPDH (Gene ID:NO_000012.12)forward primer, 5′-AGCCTC AAGATCATCAGCAATG-3′, GAPDH reverse primer, 5′-CACGATACCAA AGTTGTCATGGAT-3′. The Ct values of IL-1β and TNF-α in each sample

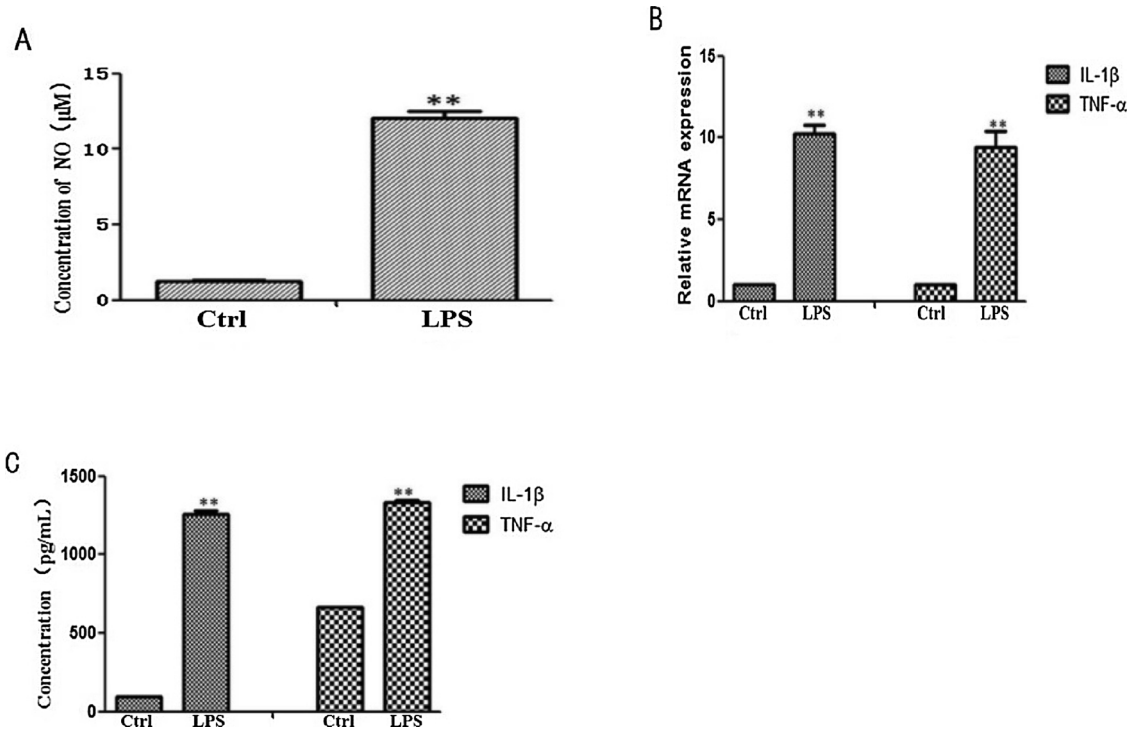

Fig. 4. Treatment with LPS induced inflammation in U937 cells. After treated with LPS, concentration of NO (A) was determined by Griess, mRNA levels of IL-1β and TNF-α (B) in U937 were determined by RT-PCR. (C) The concentrations of IL-1β and TNF-α secreted by U937 were analyzed by ELISA. **P < 0.01 versus Control group.

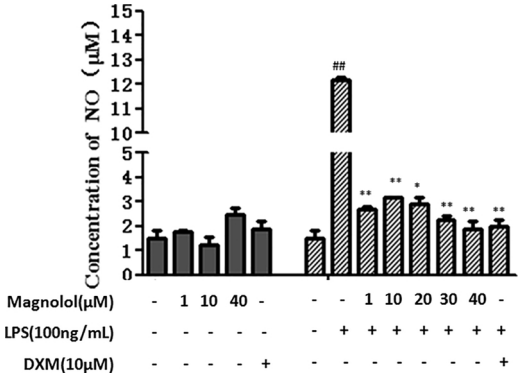

Fig. 5. Pretreatment with magnolol protected against LPS-induced inflammation. Levels of NO in U937 were analyzed by Griess Reagent. ##P < 0.01 versus LPS group, *P < 0.05 versus Control group, **P < 0.01 versus Control group.

were normalized using the values of GAPDH. The relative fold changes of target gene mRNA expression level were calculated as follow: gene relative expression = samples (Mean Ct of target gene – mean Ct of control gene)/control (average gene Ct of target gene - average gene Ct of control gene).

2.9. Western blotting assay

Cells lysed in RIPA were broken by cell scraper and heated 10 min at 100 °C. Lysates were centrifuged at 1200 rpm for 10 min, and the supernatants were collected as total protein fractions. Proteins were quantified by BCA Protein Assay Kit and equivalent protein quantities were prepared for western blotting. Proteins were separated electrophoretically by SDS-PAGE and transferred onto PVDF. The membranes were blocked with 5% non-fat dried milk for 60–120 min at room temperature. Subsequently the membranes were incubation with primary antibodies in WB antibody diluent overnight at 4 °C. After washing by TBST, the membranes were incubated with HRP-conjugated anti-rabbit or anti-mouse secondary antibodies in 5% non-fat dried milk at room temperature for 60–120 min. Washed by TBST three times for 30 min, the immunoreactivity and signals of the membranes were monitored by chemiluminescence with medical X-ray tabletting clip.

2.10. Inflammatory bowel diseases model and drug treatment

Experimental colitis mice model was induced by routine administration of DSS solution dissolved in drinking distilled water at a concentration of 2.5% (w/v) ad libitum for 8 consecutive days as previously described by Neufert(Neufert et al., 2007). Distilled water was given to mice in the normal group for the same period. The body weight of each mice was recorded daily. On day 3, the mice with significant body weight loss, diarrhea, and gross bleeding were considered as experimental candidates of colitis. All the mice with comparable disease index were then randomly divided into 5 groups (n = 8): (1) DSS model group, intragastric administrated with distilled water;(2) positive control group, DXM (5 mg/kg)intragastric administrated with distilled water;(3) high dose treatment group, intragastric administrated with magnolol (20 mg/kg);(4) medium dose treatment group, intragastric administrated with magnolol (10 mg/kg);(5) low dose treatment group, intragastric administrated with magnolol (5 mg/kg) The mice in control group received drinking water without DSS throughout the entire experimental period.

2.11. Measurement of colonic levels of cytokines

Mice colonic tissues (100 mg) were isolated and homogenized with 100 μ L RIPA lysis buffer supplemented with protease inhibitor cocktail. The supernatant was collected as total protein samples after centrifugation at 13,000 rpm at 4℃. Protein concentrations were determined using Pierce BCA Protein Assay Kit. Expression of protein levels of IL-1, IL-6 and TNF- α in the homogenates were examined using

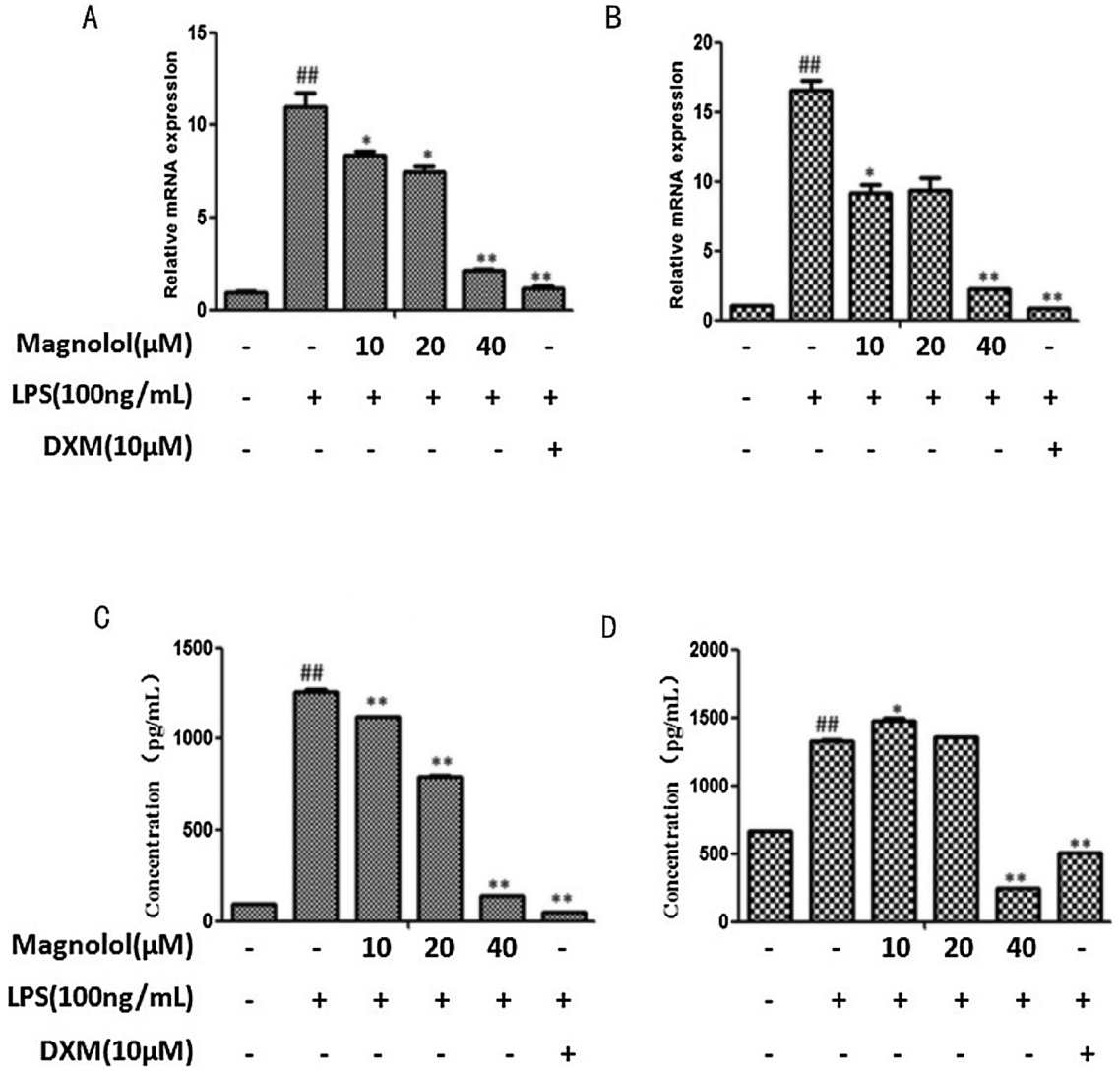

Fig. 6. Pretreatment with magnolol protected against LPS-induced IL-1β and TNF-α expression. The mRNA expressions of IL-1β (A) and TNF-α (B) were detected by RT-PCR and the concentrations of IL-1β (C) and TNF-α (D) were determined by ELISA. ##P < 0.01 versus Control group, *P < 0.05 versus LPS group, **P < 0.01 versus LPS group.

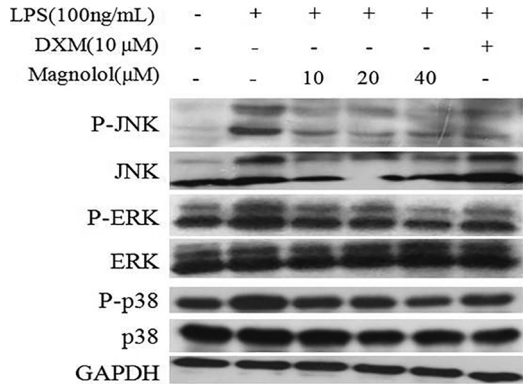

Fig. 7. Magnolol protected against inflammatory through MAPK signaling pathway on U937 cells. The expression of main proteins in MAPK signaling pathway were examed by Western blotting from normal, LPS, magnolol + LPS and DXM groups.

ELISA kits according with the standard procedures recommended. The results were normalized to the total weight of colon tissues and quantified as pg/mg.

2.12. Hematoxylin/eosin staining

Mice were euthanized with CO_2 and the colons were dissected, followed by a gentle washing with ice-cold phosphate buffered saline (PBS). Distal colons with 0.5 ~ 1 cm length were fixed in 4% paraformaldehyde for 12 h and embedded in paraffin. Colon sections were stained with hematoxylin/eosin and then subjected to blind analysis and scored as previously described(Xiao et al., 2013, Mu et al.,2016).

2.13. Statistical analysis

The experimental data were expressed as mean standard deviation (mean ± SD), and analyzed by Graphpad prism 5 software with ANOVA test and Student's *t*-test method. The experiment was repeated at three times. #P < 0.05 and *P < 0.05 were significant difference. ##P < 0.01 and **P < 0.01 were notably significant difference and datum were considered statistically significant.

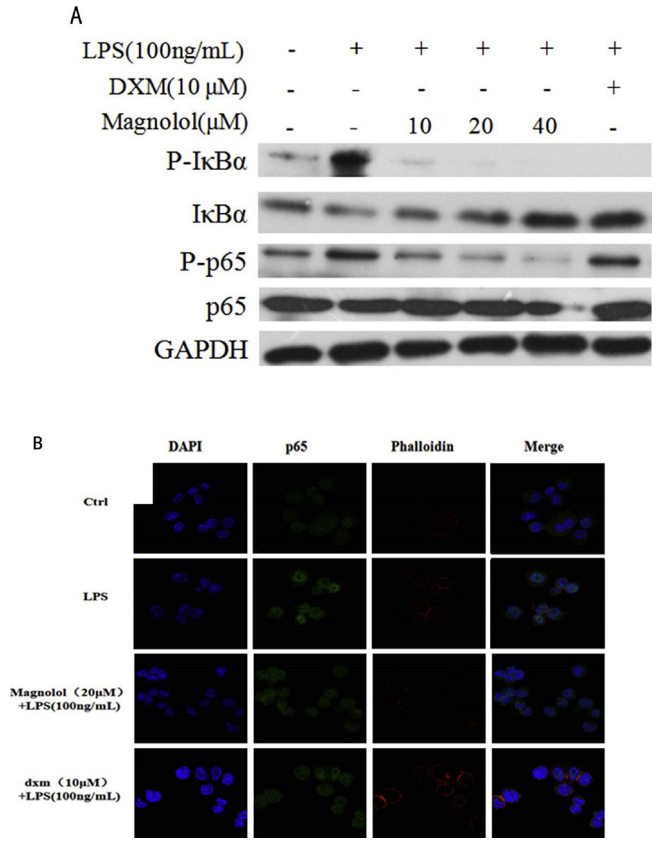

Fig. 8. Magnolol protected against inflammatory through NF-κB signaling pathway on U937 cells. The expression of main proteins in NF-κB signaling pathway were detected by Western blotting (A) and confocal microscope (B) from normal, LPS, magnolol + LPS and DXM groups.

3. Results

3.1. Effects of Magnolol on cytotoxicity in U937 and LO-2

In order to detect the toxicity of magnolol in vitro, we investigated the effects of magnolol on U937 and LO-2 human normal liver cells by MTT assay at different concentrations (10, 20, 30, 40, 50, 60, 70, 80, 90, 100 μM) for 24 h and 48 h. The results showed that the toxicity of magnolol between U937 and LO-2 was similar. The cell viability was promoted at low concentration, and the cytotoxicity of magnolol was increased with the increasing of the concentration. When the concentration of magnolol was below to 60 μM, the viability of U937 cells was significantly higher than before (Fig. 2A). When the concentration of magnolol was below to70 μM, the viability of LO-2 cells was more than 80% after treated 48 h and there was no cytotoxicity after 24 h (Fig. 2B). Therefore, in the subsequent study of magnolol on phagocytic and anti-inflammatory activity in U937 cell, we selected the non-toxic concentration (below to 60 μM) for the follow-up experiment.

3.2. Effects of Magnolol on phagocytosis in U937 cells

Phagocytosis is one of the main functions of macrophages. We used flow cytometry and confocal microscope to analyze the effect of magnolol on the ability of phagocytosis. The fluorescent microspheres swallowed by U937 cells were detected after U937 cell treated by magnolol at different concentrations (1, 10, 20, 40 μM). The green fluorescent within cells means the stronger phagocytosis of cells. As shown in Table 1, Magnolol enhanced the ability of U937 cells to engulf fluorescent microspheres in a concentration-dependent manner. In the low concentration (below to 10 μM) of cells was detected by flow cytometry(A) and confocal microscope (B). Representative immunofluorescence images were taken. Magnolol, there was no effect on the phagocytosis of U937 cells and magnolol exerted phagocytic effect in a concentration-dependent manner at 10–40 μM (Fig. 3A). The confocal microscope results showed that the fluorescence intensity of U937 cells was significantly enhanced by the addition of 20 μM magnolol (Fig. 3B).

3.3. LPS induced inflammation in U937

In our study, U937 cells were induced with 100 ng/mL LPS to cause inflammatory reaction. LPS treatment promotes proinflammatory cytokine generation in macrophages, including interleukin IL-6, IL-1β, NO and TNF-α, which triggers caspase cascade and bring death to cells(Li et al., 2017).We determined whether the cell inflammation model was established successfully by the expression levels of NO, IL-1β and TNF-α. The amount of NO production was detected by Griess Reagent after 24 h. The expression of IL-1β and TNF-α in the cells were detected by Real-time PCR after 6 h. After 12 h, the supernatant was obtained, and the changes of inflammatory cytokines IL-1β and TNF-α were detected by ELISA. We found that the amount of NO produced by the cells, the relative mRNA expression of proinflammatory cytokines IL-1β and TNF-α, the levels of proinflammatory cytokines IL-1β and TNF-α protein were increased in different degrees in the model group induced by LPS (Fig. 4). These findings suggested that U937 cell inflammation model was constructed successfully which could be used for the follow-up

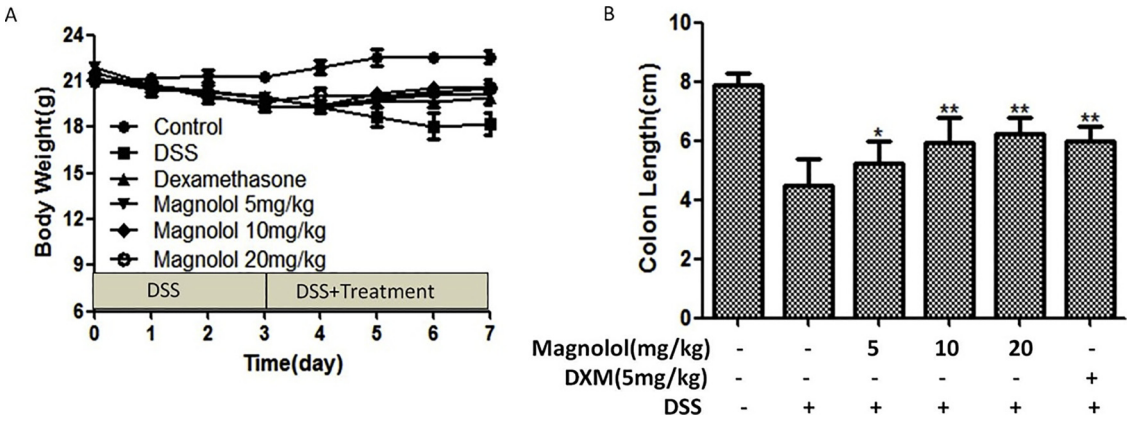

Fig. 9. The phenotypic severity of Dextran sulfate sodium (DSS)-induced colitis in mice can be effectively attenuated by 8 days after treatment with magnolol. (A) The body weight loss was significantly improved in all treatment groups versus DSS group; (B) DSS-induced shortened colon was significantly improved by high dose of magnolol and Dexamethasone. The value in the plot was expressed as means ± SEM, and statistically significant was marked by asterisk (* $p < 0.05$; ** $p < 0.01$, vs. DSS group).

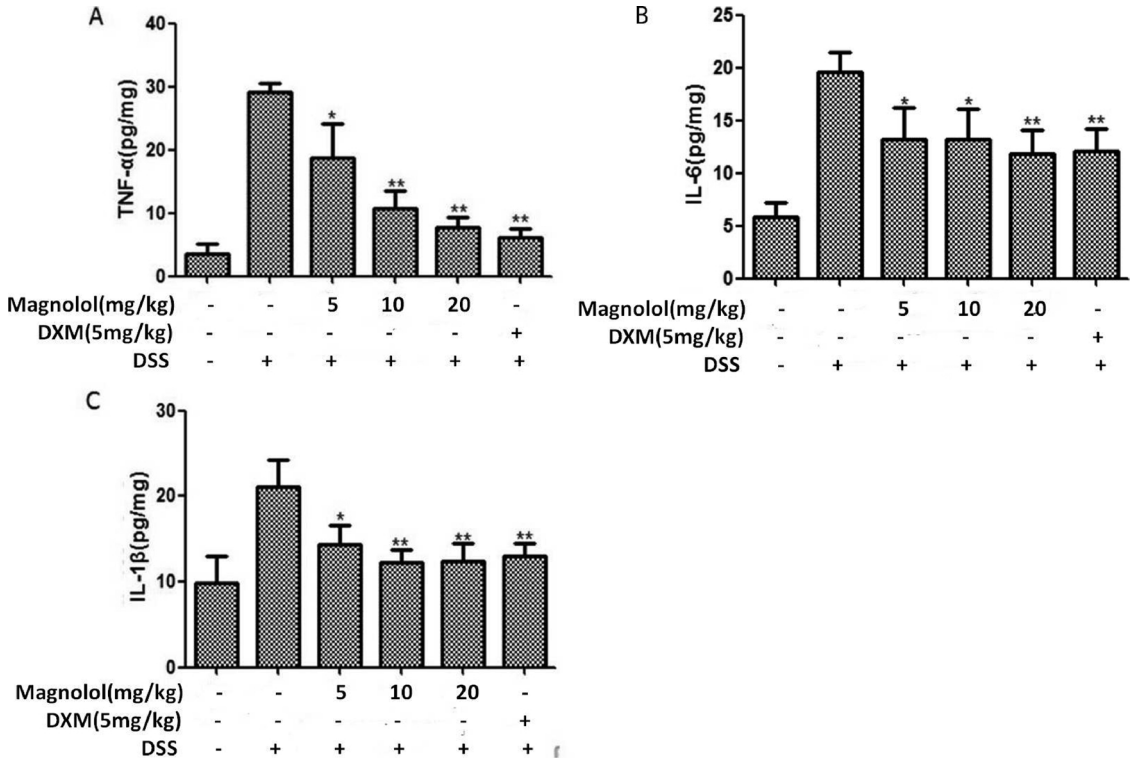

Fig. 10. 10–20 mg/kg of magnolol treatment significantly attenuated DSS-induced high levels of proinflammatory cytokines (A) TNF-α, IL-6 (B) and IL-1β(C) in the colonic tissues. The value in the plot was expressed as means ± SEM, and statistically significant was marked by asterisk.

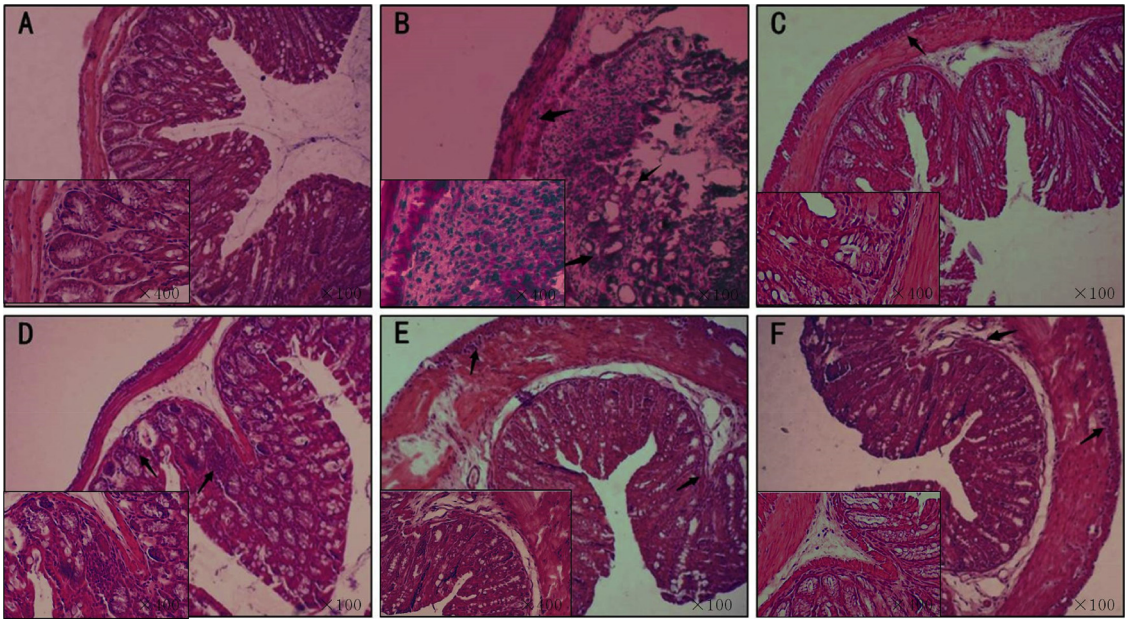

Fig. 11. 10–20 mg/kg of magnolol treatment effectively attenuated histopathological changes in the colon of DSS-treated mice with hematoxylin/eosin (H&E) staining. (A) Control group; (B) DSS group; (C) Dexamethasone group;(D) Magnolol 5 mg/kg; (E) Magnolol 10 mg/kg; (F) Magnolol 20 mg/kg.

experiments.

3.4. Magnolol ameliorates LPS-induced NO production

Induced by endotoxin and some cytokines, macrophages, involved in immune regulation and inflammatory response, can generate a lot of NO which have some toxicity on the cells, and affect the formation and release of related inflammatory factors. We used Griess Reagent to detect the effect of different concentrations of Magnolol on NO production induced by LPS in U937 cells. The results showed that, without LPS induction, different concentrations (11040 μM) of magnolol group and positive drug control DXM group (10 μM), the production of NO in U937 was not increased after treatment 24 h. LPS significantly induced NO production in U937 cells and different concentrations (110203040 μM) of magnolol and 10 μM DXM inhibited the production of LPS-induced NO production (Fig. 5).

3.5. Magnolol ameliorates LPS-induced IL-1β and TNF-α expression

To investigate the effect of magnolol at different concentrations (102040 μM) on mRNA and protein levels of IL-1β and TNF-α in U937 cells induced by LPS, Real-time PCR and ELISA were used in this study. The results showed that magnolol inhibited the mRNA expression of IL-1β and TNF-α in a concentration-dependent manner (Fig. 6A–B). U937 cells were pretreated with different concentrations of magnolol or DXM (10 μM) for 3 h and then 100 ng/mL LPS was added to induce for 12 h. The supernatant was collected for ELISA. The results showed that magnolol inhibited the expression of IL-1β in a concentration-dependent manner (Fig. 6C). When the concentration of magnolol was 10 or 20 μM, the expression of TNF-α was not significantly affected, but the expression of TNF-α was inhibited at 40 μM (Fig. 6D). Therefore, Magnolol was believed to exert anti-inflammatory effect in U937 cells.

3.6. Magnolol ameliorates LPS-induced inflammation through MAPK and NF-κB signaling pathway

To investigate the effects of magnolol at different concentrations (10, 20, 40 μM) in U937 cells induced by LPS on MAPK and NF-κB signaling pathways, we examined the main proteins of MAPK and NF-κB signaling pathways by Western blotting and confocal microscope. The results showed that Magnolol had no significant effects on ERK1/2 in MAPK signal pathway, whereas downregulated the phosphorylation of JNK and p38 (Fig. 7). Therefore, Magnolol mainly regulated the MAPK signal pathway by phosphorylating JNK and p38 in U937 cells induced by LPS.

When the cells were in resting state, p65 was located in the cytoplasm and in a state of binding to the protein I-κB.14 LPS induced phosphorylation of I-κB and released p65 into the nucleus. The p65 was activated by phosphorylation in the nucleus. We found that treated with magnolol, the phosphorylation of IκBα in NF-κB signaling pathway was inhibited and the phosphorylation level of p65 was decreased in a concentration-dependent manner (Fig. 8A). The results of confocal microscope showed that the treatment with magnolol inhibited the aggregation of p65 in U937 cells after LPS induction (Fig. 8B). Together, these data supported that magnolol may improve inflammation in damaged U937 cells through part MAPK and NF-κB signal pathways.

3.7. Effect of magnolol on DSS-treated colitis mice

C57BL/6 mice were induced with treatment of drinking water containing 2.5% DSS to develop typical symptoms of inflammatory bowel disease including body weight loss, diarrhea and rectal bleeding. After the administration of magnolol, the loss of body weight caused by DSS was significantly improved. The moderate dose of magnolol (10 mg/kg) had the greatest influence on the weight of mice (Fig. 9A). The average length of colon in DSS treatment group was significantly shorter than that in the control group. After magnolol treatment, the length of colon increased significantly and relieved colon congestion, edema and pathological damage (Fig. 9B), and this effect of this improvement is similar to that of DXM.

3.8. Effects of Magnolol on colonic pro-inflammatory cytokines in DSS-treated mice

To evaluate the related inflammatory factors of colitis after magnolol gavage administration in DSS treatment mice, the mice colon samples of all experimental group were determined by ELISA. The results showed that the cytokines of pro-inflammatory factors TNF-α (Fig. 10A), IL-6 (Fig. 10B) and IL-1β (Fig. 10C) attenuated significantly in a concentration dependent manner at the dose of 10–20 mg/kg for magnolol, and the effects of this improvement was similar to that of DXM positive control group.

3.9. Effects of Magnolol on histopathological changes a in the Colon of DSS-treated mice

The histopathological manifestations of 5–20 mg/kg after the treatment magnolol and DXM were markedly improved in the DSS-treated mice. After 8 days consumption of 2.5% DSS mice canker of the intestinal wall, severe crypt devastation, inflammatory cell infiltration (Fig. 11, arrow mark).

4. Adiscussion

Chinese herbal medicine, the natural medicine, has a very rich clinical and theoretical accumulation in the prevention and treatment of various diseases(Liu et al., 2016). It contains many active ingredients, rich and varied of structural characteristics. In the drug research or development, novel food health and other fields, thus it has great potential and as a valuable material resources(Zheng, 2017, Yao et al.,2017). There are a very rich natural products and Chinese herbal medicine resources in China. The existing compounds have been modified to obtain new drugs, which is an extremely important research direction and popular field to modernize traditional Chinese medicine(Liu and Ji, 2017).

Magnolia, widely used in the pharmaceutical industry, is an important traditional Chinese medicine. There are more than one thousand kinds of drugs with its raw materials, such as Xiangsha Yangwei pills, Huo Hong righteous gas, Ma Ren Wan, and so on. However, the high purity of magnolol and other major active ingredients of magnolia is still on development stage in the drug research and application of mostly extraction mixture(Lin et al., 2009; Matsui et al., 2009).Studies have shown that magnolol in the antibacterial, anti-inflammatory,anti-tumor, anti-oxidation, protection of cardiovascular and cerebrovascular, analgesic and other aspects exerted a potential development value(Wah et al., 2008; Saito et al., 2008).At present, the immunological activity and anti-inflammatory activity of magnolol have achieved progress. However, there are still single research models *in vitro* and *in vivo*, the clinical directivity is not enough. The mechanism of action and the target are still lack of systematic research and verification. In our study, we established the human macrophage inflammation model inflammatory bowel disease model. Magnolol on immune function, anti-inflammatory activity and mechanism of action were verified in the study.

Firstly, U937 cells and LO-2 normal liver cells are employed to detect the cytotoxicity of Magnolol. Our results showed that at the concentration of 0–60 μM, there was not toxicity effects of Magnolol to U937 and LO-2. Therefore, we chose below to 60 μM of Magnolol to futher experiments. Massive evidence in experimental and clinical studies performed on immune proved that magnolol contributes to phagocytosis(Chen et al., 2017, Choi et al.,2015).Our results showed that the phagocytosis of U937 cells could be enhanced in a magnolol concentration-dependent manner, suggesting that magnolol enhanced the ability of recognization and swallowing pathogens when pathogenic microorganisms were invaded and removement necrotic disintegrated cell debris from inflammatory tissue.

In addition to phagocytosis, there are reports indicating a key impact of anti-inflammation mediated by magnolol(Lin et al., 2007).NO, IL-1β and TNF-α, effective biochemical markers of inflammatory are employed to observe inflammation level.The increased level of NO, IL-1β and TNF-α, a reliable index for inflammation, demonstrated that we successfully to establish the inflammatory modal for U937 cells. We found that magnolol exhibited anti-inflammatory activity by decreasing both mRNA and protein levels of NO, IL-1β and TNF-α. It is well-known that MAPK and NF-κB signaling pathways have been implicated in inflammation(Sun et al., 2017).Therefore, we make further investigation to whether MAPK and NF-κB signaling pathways were due in part in anti-inflammation mediated by magnolol. We demonstrated that magnolol down-regulated the phosphorylation of JKK and p38 in MAPK

signaling pathway and down-regulated the phosphorylation levels of IκBα and p65 in NF-κB signaling pathway to exert anti-inflammatory activity.

Mitogen-activated protein kinase (MAPK) is a highly conserved serine/threonine protein kinase family that plays inportant role in many basic cellular processes, including proliferation, differentiation, motility, stress response, apoptosis and survival. Conventional MAPKs include extracellular signal-regulated kinases 1 and 2 (Erk1/2 or p44/42), c-Jun amino-terminal kinase 1–3 (JNK1–3) / stress-activated protein kinases (SAPK1A, 1B, 1C), p38 isomers (p38a, beta, gamma and delta) and Erk5(Arthur and Ley, 2013; Cargnello and Roux, 2011; Cseh et al., 2014; Darling and Cook, 2014; Koul et al., 2013; Plotnikov et al., 2011; Sehgal and Ram, 2013).Therefore, the crosstalk between MAPK and NF-κB pathway transduction during the course of inflammation with magnolol needs to be further studied.

Funding

This project were supported by the National Natural Science Foundation of China (NSFC) (81573607, 81202917), Science and Technology Planning Project of Guangdong Province (2015A020211036).

Conflict of interest

The authors declare no competing financial interest.

Acknowledgments

We also give great thanks to Rebecca Meyer, Ziqian Li and Xinmin Li for good recommends and reviews for this paper.

References

Arthur, J.S., Ley, S.C., 2013. Mitogen-activated protein kinases in innate immunity. Nat. Rev. Immunol. 13, 679–692. https://doi.org/10.1038/nri3495.

Gabay, C., Kushner, I., 1999. Acute-phase proteins and other systemic responses to inflammation. N. Engl. J. Med. 340, 448–454. https://doi.org/10.1056/NEJM199902113400607.

Cargnello, M., Roux, P.P., 2011. Activation and function of the MAPKs and their substrates, the MAPK-activated protein kinases. Microbiol. Mol. Biol. Rev. 75, 50–83. https://doi.org/10.1128/MMBR.00031-10.

Chen, H., Liu, X., Clayman, E.S., Shao, F., Xiao, M., Tian, X., Fu, W., Zhang, C., Ruan, B., Zhou, P., 2015. Synthesis and evaluation of a CBZ-AAN-Dox prodrug and its in vitro effects on SiHa cervical Cancer cells under hypoxic conditions. Chem. Biol. Drug Des. 86, 589–598. https://doi.org/10.1111/cbdd.12525.

Chen, X., Hu, Y., Shan, L., Yu, X., Hao, K., Wang, G.X., 2017. Magnolol and honokiol from Magnolia officinalis enhanced antiviral immune responses against grass carp reovirus in Ctenopharyngodon idella kidney cells. Fish Shellfish Immunol. 63, 245–254. https://doi.org/10.1016/j.fsi.2017.02.020.

Choi, E.J., Kim, H.I., Kim, J.A., Jun, S.Y., Sang, H.K., Dong, J.P., Son, S.J., Kim, Y., Shin, O.S., 2015. The herbal-derived honokiol and magnolol enhances immune response to infection with methicillin-sensitive Staphylococcus aureus (MSSA) and methicillin-resistant S. Aureus (MRSA). Appl. Microbiol. Biotechnol. 99, 4387–4396. https://doi.org/10.1007/s00253-015-6382-y.

Cseh, B., Doma, E., Baccarini, M., 2014. "RAF" neighborhood: protein–protein interaction in the Raf/Mek/Erk pathway. FEBS Lett. 588, 2398–2406. https://doi.org/10.1016/j.febslet.2014.06.025.

Darling, N.J., Cook, S.J., 2014. The role of MAPK signalling pathways in the response to endoplasmic reticulum stress. Biochim. Biophys. Acta 1843, 2150–2163. https://doi.org/10.1016/j.bbamcr.2014.01.009.

Doherty, G.J., Mcmahon, H.T., 2009. Mechanisms of endocytosis. Annu Rev Biochem. Annu Rev Biochem 78, 857–902. https://doi.org/10.1146/annurev.biochem.78.081307.110540.

Farghadan, M., Ghafoori, H., Vakhshiteh, F., Shahzadeh Fazeli, S.A., Farzaneh, P., Kokhaei, P., 2016. The effect of Artemisia fragrans willd: essential oil on inducible nitric oxide synthase gene expression and nitric oxide production in lipopolysaccharide-stimulated murine macrophage cell line. Iran. J. Allergy Asthma Immunol. 15, 515–524.

Fujiwara, N., Kobayashi, K., 2005. Macrophages in inflammation. Curr. Drug Targets Inflamm. Allergy 4, 81–286. https://doi.org/10.2174/1568010054022024.

Hansson, G.K., 2005. Inflammation, atherosclerosis, and coronary artery disease. N. Engl. J. Med. 352, 429–430. https://doi.org/10.1056/NEJMra043430.

Huang, G., Shi, L.Z., Chi, H., 2009. Regulation of JNK and p38 MAPK in the immune system: signal integration, propagation and termination. Cytokine 48, 161–169. https://doi.org/10.1016/j.cyto.2009.08.002.

Killeen, M.J., Linder, M., Pontoniere, P., Crea, R., 2014. NF-κβ signaling and chronic inflammatory diseases: exploring the potential of natural products to drive new therapeutic opportunities. Drug Discov. Today 19, 373–378. https://doi.org/10.1016/j.drudis.2013.11.002.

Koul, H.K., Pal, M., Koul, S., 2013. Role of p38 MAP kinase signal transduction in solid tumors. Genes Cancer 4, 342–359. https://doi.org/10.1177/1947601913507951.

Lawrence, T., Gilroy, D.W., Colville-Nash, P.R., Willoughby, D.A., 2001. Possible new role for NF-kappaB in the resolution of inflammation. Nat. Med. 7, 1291. https://doi.org/10.1038/nm1201-1291.

Li, J., Zhong, L., Zhu, H., Wang, F., 2017. The protective effect of Cordycepin on D-Galactosamine/Lipopolysaccharide-Induced acute liver injury. Mediators Inflamm. 28. https://doi.org/10.1155/2017/3946706. 3946706.

Lin, Y.R., Chen, H.H., Ko, C.H., Chan, M.H., 2007. Effects of honokiol and magnolol on acute and inflammatory pain models in mice. Life Sci. 81https://doi.org/10.1016/j.lfs.2007.08.014. 1071-8.

Lin, Y.R., Chen, H.H., Lin, Y.C., Ko, C.H., Chan, M.H., 2009. Antinociceptive actions of honokiol and magnolol on glutamatergic and inflammatory pain. J. Biomed. Sci. 16, 94. https://doi.org/10.1186/1423-0127-16-94.

Liu, B.C., Ji, G., 2017. Sparking thinking: studying modern precision medicine will accelerate the progression of traditional chinese medicine patterns. J. Altern. Complement. Med. 23, 502. https://doi.org/10.1089/acm.2016.0383.

Liu, M., Wang, Y., Liu, Y., Ruan, R., 2016. Bioactive peptides derived from traditional Chinese medicine and traditional Chinese food: a review. Food Res. Int. 89, 63. https://doi.org/10.1016/j.foodres.2016.08.009.

Rabinovitch, Michel, 1995. Professional and non-professional phagocytes: an introduction. Trends Cell Biol. 5, 85. https://doi.org/10.1016/s0962-8924(00)88955-2.

Matsui, N., Takahashi, K., Takeichi, M., Kuroshita, T., Noguchi, K., Yamazaki, K., Tagashira, H., Tsutsui, K., Okada, H., Kido, Y., 2009. Magnolol and honokiol prevent learning and memory impairment and cholinergic deficit in SAMP8 mice. Brain Res. 1305, 108. https://doi.org/10.1016/j.brainres.2009.09.107.

Mu, H.X., Jing, L., Fatima, S., Lin, C.Y., Shi, X.K., Du, B., Xiao, H.T., Fan, B.M., Bian, Z.X., 2016. Anti-inflammatory actions of (+)-3′α-Angeloxy-4′-keto-3′,4′-dihydroseselin (Pd-Ib) against dextran sulfate sodium-induced colitis in C57BL/6 mice. J. Nat. Prod. 79, 1056. https://doi.org/10.1021/acs.jnatprod.5b01071.

Neufert, C., Becker, C., Neurath, M.F., 2007. An inducible mouse model of colon carcinogenesis for the analysis of sporadic and inflammation-driven tumor progression. Nat. Protoc. 2, 1998. https://doi.org/10.1038/nprot.2007.279.

Ovchinnikov, D.A., 2010. Macrophages in the embryo and beyond: much more than just giant phagocytes. Genesis 46, 447–462. https://doi.org/10.1002/dvg.20417.

Pang, Y.L., Han, X.F., Bamikole, M.A., Gong, Z.H., Tang, S.X., Tan, Z.L., Xiao, W.J., Zhou, C.S., Wang, M., Deng, Y.L., 2013. Anti-diarrhea and anti-oxidant properties of Magnolol. Trop. J. Pharm. Res. 12, 85–91. https://doi.org/10.4314/tjpr.v12i1.14.

Park, H.J., Song, M., 2017. Leaves of Raphanus sativus L. Shows anti-inflammatory activity in LPS-Stimulated macrophages via suppression of COX-2 and iNOS expression. Prev. Nutr. Food Sci. 22, 50–55. https://doi.org/10.3746/pnf.2017.22.1.50.

Park, S.Y., Yi, E.Y., Jung, M., You, M.L., Kim, Y.J., 2011. Ethyl pyruvate, an anti-inflammatory agent, inhibits tumor angiogenesis through inhibition of the NF-κB signaling pathway. Cancer Lett. 303, 150–154. https://doi.org/10.1016/j.canlet.2010.12.024.

Plotnikov, A., Zehorai, E., Procaccia, S., Seger, R., 2011. The MAPK cascades: signaling components, nuclear roles and mechanisms of nuclear translocation. Biochim. Biophys. Acta 1813, 1619–1633. https://doi.org/10.1016/j.bbamcr.2010.12.012.

Robinson, M.J., Cobb, M.H., 1997. Robinson MJ, cobb MHMitogen-activated protein kinase pathways. Curr. Opin. Cell Biol. 9, 180–186. https://doi.org/10.1016/S0955-0674(97)80061-0.

Saito, J., Shibuya, K., Nagase, H., 2008. Anti-clastogenic effect of magnolol on benzo(a)pyrene-induced clastogenicity in mice. Food Chem. Toxicol. 46, 694. https://doi.org/10.1016/j.fct.2007.09.097.

Schroeder, B.R., Ghare, M.I., Bhattacharya, C., Paul, R., Yu, Z., Zaleski, P.A., Bozeman, T.C., Rishel, M.J., Hecht, S.M., 2014. The disaccharide moiety of bleomycin facilitates uptake by cancer cells. J. Am. Chem. Soc. 136, 13641–13656. https://doi.org/10.1021/ja507255g.

Sehgal, V., Ram, P.T., 2013. Network motifs in JNK Signaling. Genes Cancer 4, 409–413. https://doi.org/10.1177%2F1947601913507577.

Shao, F.Y., Du, Z.Y., Ma, D.L., Chen, W.B., Fu, W.Y., Bi-Bo, R., Wen, R., Zhang, J.X., Sheng, W., Sum, W.N., 2015. B5, a thioredoxin reductase inhibitor, induces apoptosis in human cervical cancer cells by suppressing the thioredoxin system, disrupting mitochondrion-dependent pathways and triggering autophagy. Oncotarget 6, 30939–30956. https://doi.org/10.18632/oncotarget.5132.

Sun, Y.P., Mei, L.J., Kang, N.J., Park, G., Choi, Y.W., 2017. Anti-inflammatory effects of novel polygonum multiflorum compound via inhibiting NF-κB/MAPK and upregulating the Nrf2 pathways in LPS-stimulated microglia. Neurosci. Lett. 651. https://doi.org/10.1016/j.neulet.2017.04.057.

Wah, C.L., Cheah, E.L., Saw, C.L., Wanyu, W., Heng, P.W., 2008. Antimicrobial and antioxidant activities ofCortex Magnoliae Officinalisand some other medicinal plants commonly used in South-East Asia. Chin. Med. 3, 1–10. https://doi.org/10.1186%2F1749-8546-3-15.

Wang, S.-M., Lee, L.-J., Huang, Y.-T., Chen, J.-J., Chen, Y.-L., 2000. Magnolol stimulates steroidogenesis in rat adrenal cells. Br. J. Pharmacol. 131, 1172–1178. https://doi.org/10.1038/sj.bjp.0703669.

Wang, Y., Wang, K., Huang, H., Gu, X., Teng, X., 2017. Alleviative effect of selenium on inflammatory damage caused by lead via inhibiting inflammatory factors and heat shock proteins in chicken testes. Environ. Sci. Pollut. Res. Int. 24, 1–9. https://doi.org/10.1007/s11356-017-8785-z.

Xiao, H.T., Lin, C.Y., Ho, D.H., Peng, J., Chen, Y., Tsang, S.W., Wong, M., Zhang, X.J.,

Zhang, M., Bian, Z.X., 2013. Inhibitory effect of the gallotannin corilagin on dextran sulfate sodium-induced murine ulcerative colitis. J. Nat. Prod. 76https://doi.org/10.1021/np4006772. 2120-5.

Yao, L., Chen, Y., Wang, X., Shi, X., Wang, Y., Guo, T., Yang, K., 2017. Appraising the quality of clinical practice guidelines in traditional Chinese medicine using AGREE II instrument: a systematic review. Int. J. Clin. Pract. 71. https://doi.org/10.1111/ijcp.12931.

Ying, H., Xiang, Y., Tianrui, X.U., Kong, Q., Zhang, Y., Shen, Y., Wei, Y., Wang, G., Chang, K.J., 2016. Overcoming resistance to TRAIL-induced apoptosis in solid tumor cells by simultaneously targeting death receptors, c-FLIP and IAPs. Int. J. Oncol. 49, 153–163. https://doi.org/10.3892/ijo.2016.3525.

Fong, Y.M., Marano, M.A., Moldawer, L.L., Wei, H., Calvano, S.E., Kenney, J.S., Allison, A.C., Cerami, A., Shires, G.T., Lowry, S.F., 1990. The acute splanchnic and peripheral tissue metabolic response to endotoxin in humans. J. Clin. Invest. 85, 1896–1904. https://doi.org/10.1172/jci114651.

Zhao, L., Xiao, H.T., Mu, H.X., Huang, T., Lin, Z.S., Zhong, L., Zeng, G.Z., Fan, B.M., Lin, C.Y., Bian, Z.X., 2017. Magnolol, a natural polyphenol, attenuates dextran sulfate sodium-induced colitis in mice. Molecules 22, 1218. https://doi.org/10.3390/molecules22071218.

Zheng, H., 2017. [Changes of the guangdong professional school of traditional chinese medicine in early new China]. Zhonghua Yi Shi Za Zhi 47, 91. https://doi.org/10.3760/cma.j.issn.0255-7053.2017.02.007.